European Rotorcraft Forum

COMPUTATIONALLY EFFICIENT AND HIGH FIDELITY OPTIMIZATION OF ROTOR BLADE GEOMETRY

Masahiko Sugiura, Yasutada Tanabe,
Japan Aerospace Exploration Agency
6-13-1 Osawa, Mitaka, Tokyo, 181-0015
Japan

Hideaki Sugawara
Ryoyu Systems Co., LTD.
6-19 Oe-Cho, Minato-ku, Nagoya, Aichi, 455-0024
Japan

Masahiro Kanazaki
Tokyo Metropolitan University
6-6 Asahigaoka, Hino, Tokyo, 191-0065
Japan

Abstract

This paper explains a computationally efficient and high fidelity optimization method. CFD technique to get aerodynamic solution and optimization technique to obtain optimized blade geometry are weakly coupled. The base CFD code herein is a structured grid solver, rFlow3D, which has intensively been developed for helicopter applications at Japan Aerospace Exploration Agency. The rFlow3D is a highly versatile CFD code that can numerically simulate flows around helicopter in a wide range of flow conditions, considering trimming and blade elastic deformation. For optimization, Genetic Algorithm is combined with Kriging model. Blade geometry is expressed with a few parameters by interpolating cubic spline. In this study, blade geometry optimization is conducted assuming hovering UAVs. And the optimal blade geometry is reasonably predicted, showing uniform induced velocity distribution on the rotor plane. As a next step, we plan to conduct multi-objective optimization of blade geometry, considering both forward flight and hovering in the near future.

1. INTRODUCTION

Recently, optimization techniques have been applied to high fidelity numerical methods such as CFD in the helicopter field since sophisticated optimization techniques enable us to run optimization efficiently. Especially, the optimization method that combines Genetic Algorithm with Kriging model is robust for multi-modal problems and computationally efficient since a surrogate model is updated by using expected improvement values. For example, blade planform was designed to reduce high speed impulsive noise by using this optimization method [1, 2]. In other instances, blade twist distribution at the blade tip was optimized using the hybrid method of CFD and prescribed wake model [3].

On the other hand, unmanned aerial vehicles (UAVs) whose rotor radii are in the order of one meter have been popular in pesticide spraying. In particular, RMAX developed by YAMAHA Motor Co., Ltd. is widely used in Japan (Figure 1). Table 1 shows its major specifications. The main rotor diameter is approximately three meter and it is designed to be carried by automobile. This UAV is mainly used in nearly hovering (usually at very low flight speed: approximately 5 m/s) to spray pesticide.

Thus, an objective of this study is obtaining optimal blade geometry for hovering, considering this UAV's size.

Figure. 1: YAMAHA RMAX [4].

Table 1: YAMAHA RMAX Specifications [4].

Main rotor diameter	3.13 m
Overall length	2.75 m
Overall width	0.72 m
Overall height	1.08 m

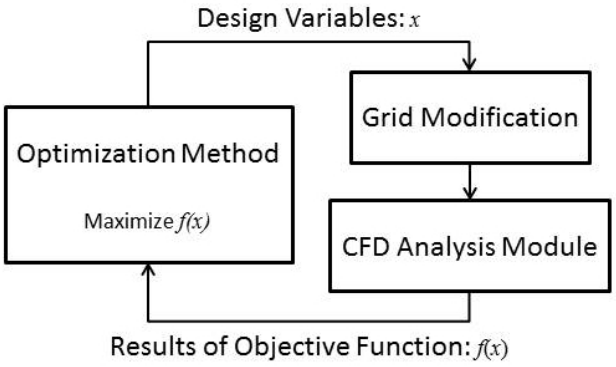

Figure 2: Diagram of optimization procedure.

2. NUMERICAL METHODS

2.1. Optimization Method

2.1.1 Optimization Procedure

For the modification of blade geometry to maximize hovering efficiency, optimization technique is combined with CFD flow solver. In the present research, CFD technique to get aerodynamic solution and optimization technique to obtain optimized blade geometry are weakly coupled. Figure 2 shows the diagram of optimization procedure in the present paper. Grid for CFD analysis is modified using blade geometry design variables which are suggested by the optimization method. The results of CFD analysis is used to evaluate the objective functions for optimization process.

For optimization, Genetic Algorithm is combined with Kriging model. The details of GA and Kriging model are described in [5, 6].

2.1.2 Generic Algorithm (GA)

Genetic algorithms (GA) [7] are a searching mechanism based on natural selection and genetics. GAs use the objective function value itself, not its derivative information. This feature makes GAs robust and attractive to the aerodynamic design problems where non-linearity, multi-modality and discontinuities may exist. Another merit of GAs is that they search the optimum point from a population of points, not a single point. It makes GAs the promising methods for multi-objective (MO) problems.
Once the optimization is over, the validity of the search region is examined using Kriging model.

2.1.3 Kriging Model

The Kriging model expresses the unknown function $y(\mathbf{x})$ as

$$y(\mathbf{x}) = \beta + Z(\mathbf{x}) \quad (1)$$

where, $\mathbf{x}$ is an *m*-dimensional vector (*m* design variables), β is a constant global model and $Z(\mathbf{x})$ represents a local deviation at an unknown point, $\mathbf{x}$, is expressed using stochastic processes. The sample points are interpolated with the Gaussian random function as the correlation function to estimate the trend of the stochastic processes.

2.1.4 Expected Improvement

Expected Improvement (EI) [8] means the potential of being superior to current optimum. EI considers the predicted function value and its uncertainty at the same time. Thus, in the maximization problem, the solution with small objective function value and large uncertainty may be larger than the solution with large objective function and small uncertainty. This feature makes it possible to explore the design space globally.
In this study, EI of objective function is directly used as fitness values in the optimization. GA maximizes EIs of objective functions to finds the non-dominated solutions about EIs and several points are selected from the non-dominated solutions to update the Kriging model. Overall procedure of the optimization is shown in Figure 3.

2.2 CFD

CFD solver for rotorcraft (rFlow3D) has been enthusiastically developed at Japan Aerospace Exploration Agency (JAXA). The rFlow3D is a highly versatile CFD code that can numerically simulate flows around helicopter in a wide range of flow conditions, considering trimming and blade elastic deformation. The governing equation of *rFlow3D* is a three dimensional compressible Euler equation:

$$\frac{\partial}{\partial t}\int_{V(t)} \mathbf{U}\,\mathrm{d}V + \int_{S(t)} \mathbf{F}\cdot\mathbf{n}\mathrm{d}S = 0 \quad (2)$$

where **U** is a solution vector, **F** is a velocity vector for x, y, z directions, **n** is a unit normal vector. Components of **U** and **F** are as follows:

$$\mathbf{U} = \begin{pmatrix} \rho \\ \rho\mathbf{v} \\ \rho e \end{pmatrix}, \quad \mathbf{F} = \begin{pmatrix} (\mathbf{v}-\dot{\mathbf{x}})\cdot\mathbf{n}\rho \\ (\mathbf{v}-\dot{\mathbf{x}})\cdot\mathbf{n}\rho\mathbf{v} + p\mathbf{n} \\ (\mathbf{v}-\dot{\mathbf{x}})\cdot\mathbf{n}\rho e + p\mathbf{v}\cdot\mathbf{n} \end{pmatrix} \quad (3)$$

v is a velocity vector for x, y, z directions, $\dot{\mathrm{x}}$ is a velocity vector of moving cell boundary, ρ is air density, *p* is pressure, and *e* is total energy.

Finite volume method and moving overlapped grid method are used in this numerical solution. mSLAU (modified Simple Low-dissipation AUSM) [9] which is modified for applying all-speed SLAU scheme to moving overlapped grid method is used for numerical velocity, and fourth spatial precision FCMT (Fourth-order Compact MUSCL TVD) scheme [10] is used for reconstruction of physical values. For time integration, fourth-order Runge-Kutta method is used in background orthogonal grid, and dual-time stepping method [11] is used in blade and fuselage grids to construct unsteady implicit method. LU-SGS/DP-LUR is used for simulated time integration. Tri-Linear interpolation method is used for exchange of values among grids.

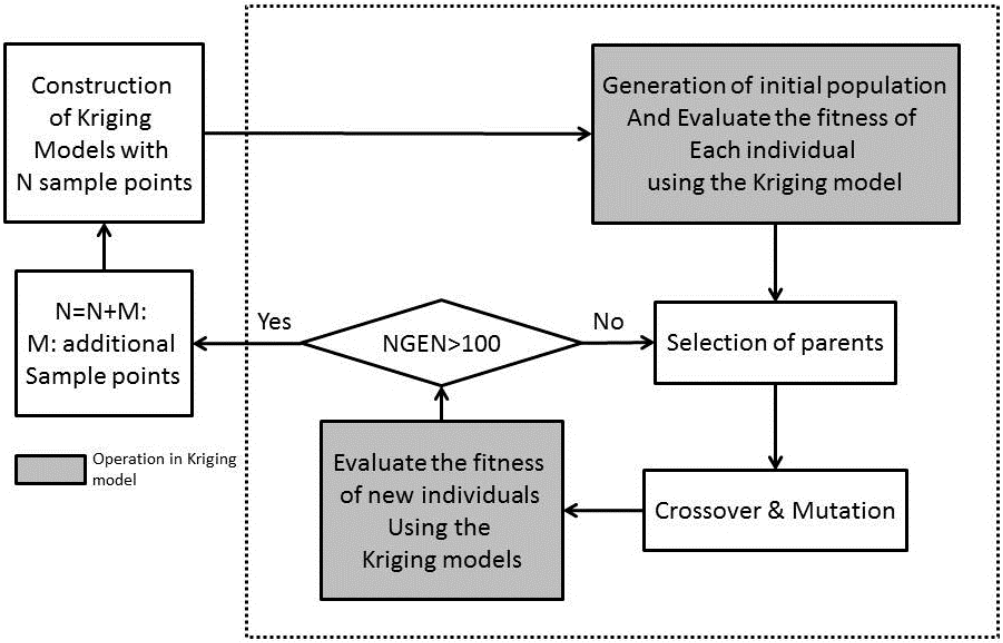

Figure 3: Overall procedure of the optimization.

3. NUMERICAL CONDITIONS

JAXA conducted wind tunnel tests of a rotor with an active flap to evaluate its BVI (Blade Vortex Interaction) noise reduction effect in 2012 and 2013 (Figures 4, 5). The span length of the blade is almost the same as RMAX. This blade is named as the base blade in the following sections to distinguish other blade geometries. The wind tunnel test condition of hovering is summarized in Table 2. This condition is adopted as a numerical condition in this study.

Table 3 summarizes design variables for blade geometry optimization. Span positions of design variables are shown in Figure 6. Twist and chord length are selected as design variables and distributions of them are interpolated by cubic splines.

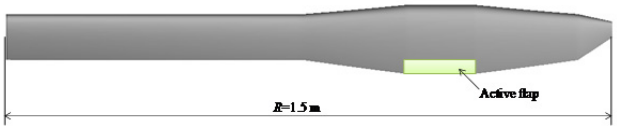

Figure 4: Geometry of a blade with an active flap.

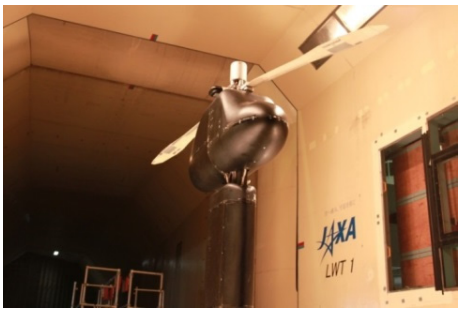

Figure 5: Active flap wind tunnel test setup.

Table 2: Active flap wind tunnel test condition.

Airfoil	NACA23012
Number of blades	2
Span length	1.5 m
Revolution	1273 RPM
Tip Mach number	0.588
Thrust	1176 N

Table 3: Design variables for blade geometry optimization.

Design Variables	*Constraint Conditions*
Twist at root	-15 deg ~ +15 deg
Twist at tip	-15 deg ~ +15 deg
Chord length at tip	0.2 c ~ 2.0 c
Span position of twist control	0.4 R ~ 0.8 R
Twist at the span positon of twist control	-15 deg ~ +15 deg
Span position of chord length control	0.4 R ~ 0.8 R
Chord length at the span position of chord length control	0.5 c ~ 2.0 c

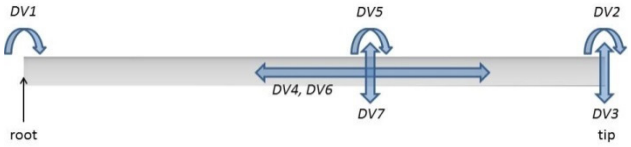

Figure 6: Span positions of design variables.

As an objective function, figure of merit (FM) is selected since maximizing hovering efficiency helps

decreasing fuel consumption.

4. NUMERICAL RESULTS

4.1. Optimal Blade Geometry

Firstly, as an initial sample points, thirty six random blade geometries are evaluated by CFD. Then an initial guess of the optimal blade is conducted based on the Kriging model. Next, by adding sample points, Kriging model and EI map is updated. Figure 7 shows the optimization results. In the optimization process, FM reaches maximum though some points indicate lower values. FM of the base blade (Figure 4) is also shown by a dashed line in Figure 7. From this figure, it is found that FM of the base blade is high, comparing with other sample points.
As a comparison, blade geometry of the lowest FM is shown in Figure 8. Figures 9 and 10 show its twist and chord length distribution, respectively.
The optimal blade geometry is shown in Figure 11. Its twist and chord length distributions are described in Figures 12 and 13. The twist approximately linearly decreases along the span. On the other hand, the chord length gradually increases from the root to the center and drastically decreases from the center to the tip. This geometry suggests required torque is decreased by shortening the chord length of the tip.

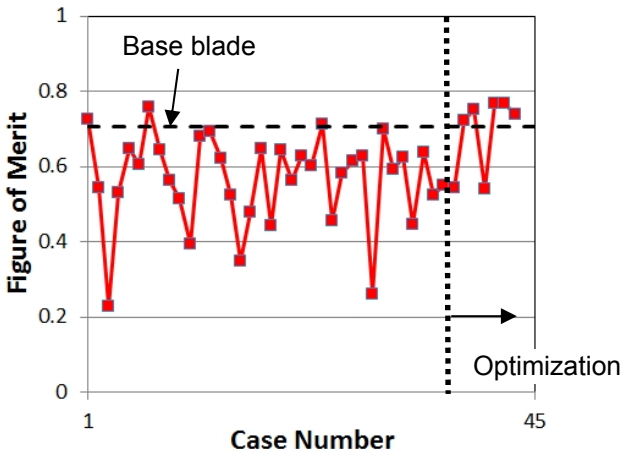

Figure 7: Optimization results.

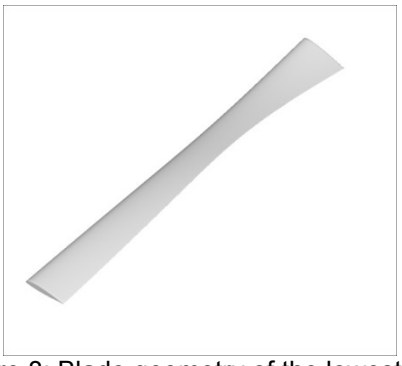

Figure 8: Blade geometry of the lowest FM.

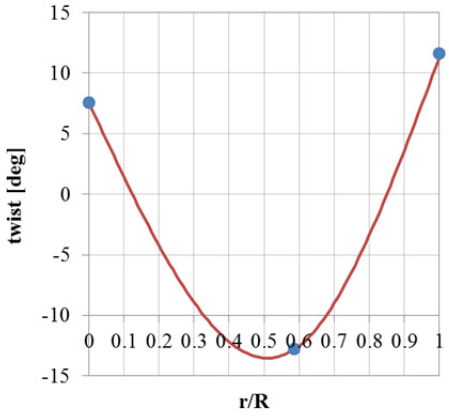

Figure 9: Twist distribution of the lowest FM blade.

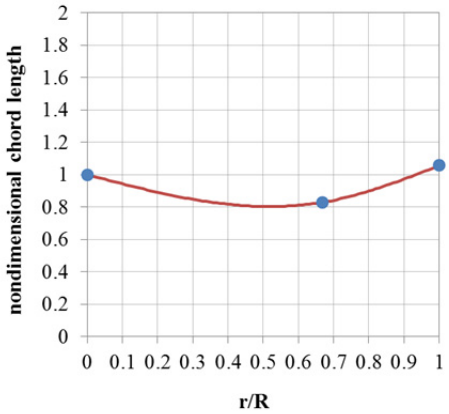

Figure 10: Chord length distribution of the lowest FM blade.

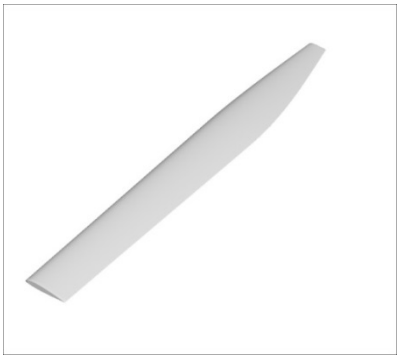

Figure 11: Optimal blade geometry.

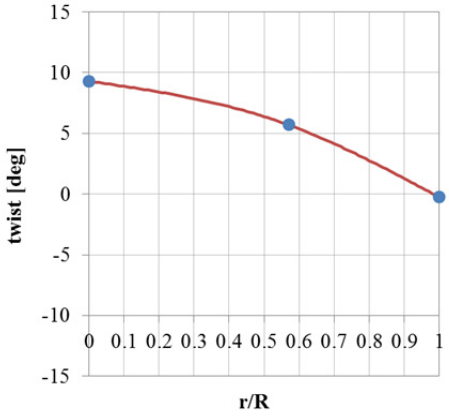

Figure 12: Twist distribution of the optimal blade.

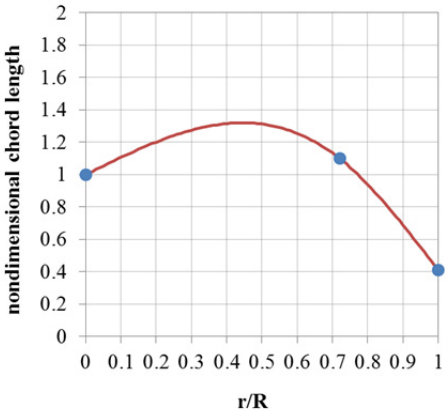

Figure 13: Chord length distribution of the optimal blade.

4.2. Induced Velocity Distribution

The vertical velocity distributions of the lowest FM blade and the optimal blade are shown in Figures 14 and 15, respectively. Blue color indicates downwash and red color indicates upwash. Comparing these two figures, we can see the vertical velocity distribution of the optimal blade is more uniform than that of the lowest FM blade. That agrees with the commonly accepted knowledge that uniform velocity gives the best performance.

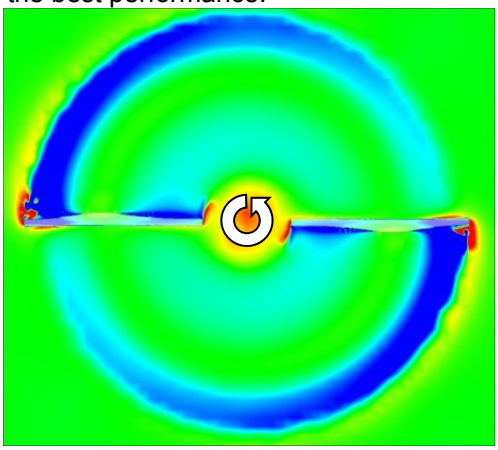

Figure 14: Vertical velocity distribution of the lowest FM blade.

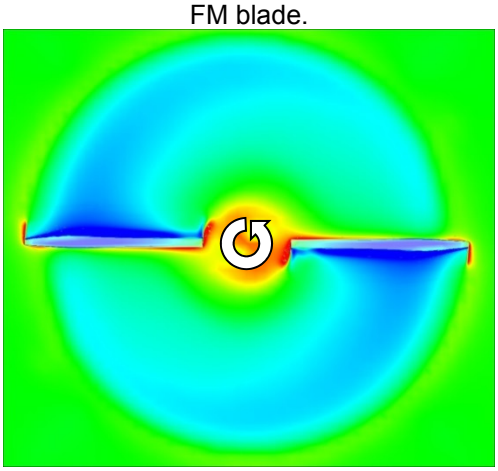

Figure 15: Vertical velocity distribution of the optimal blade.

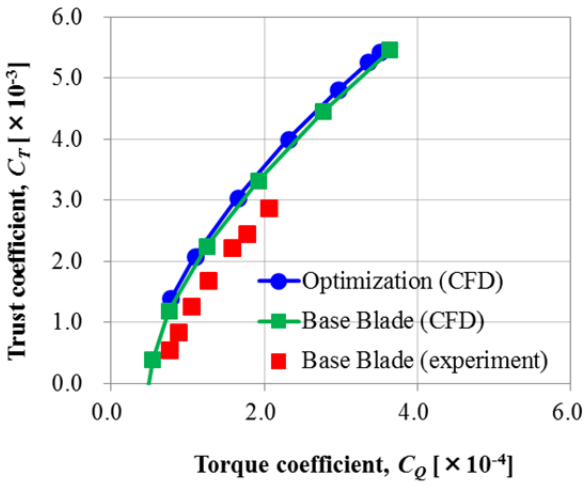

Figure 16: Relationship between the torque coefficient and the thrust coefficient.

4.3. Rotor Performance of the Optimal Blade

The relationship between the torque coefficient and the thrust coefficient, in other words, the rotor performance is shown in Figure 16. Blue, green and red symbols indicate CFD result of the optimal blade, that of the base blade and the experimental result of the base blade, respectively. From this figure, it is found that the rotor performance of CFD is higher than that of experiment since Euler solver does not consider viscous effect. We can also see from this figure that CFD predicts the rotor performance with high precision and the rotor performance of the base blade is nearly close to the optimal blade. Thus, the base blade turns out to be highly efficient in hovering.

5. CONCLUDING REMARKS

In this study, the computationally efficient and high fidelity optimization method which combines Genetic Algorithm with Kriging model is applied to the rotor blade geometry in hovering, considering pesticide spraying UAVs. Through this optimization, the optimal blade geometry is successfully obtained. And its induced velocity distribution shows the reasonable uniform flow. In terms of rotor performance, the base blade shows nearly close performance to the optimal blade. Thus, both blades turn out to be aerodynamically efficient for hovering.

FM is selected as an objective function to maximize hovering efficiency in this study. Multi-objective optimization will be conducted in the near future considering both forward flight and hovering.

REFERENCES

[1] Yang, C., et. al., “Blade Planform Optimization to Reduce HIS Noise of Helicopter in Hover, ” the American Helicopter Society 64th Annual Forum, 2008.

[2] Chae, S., et. al., “Blade Shape Optimization for Aero-Acoustic Performance Improvement of Helicopter in Hover,” the American Helicopter Society 65th Annual Forum, 2009.

[3] Takeda, S., et. al., “Evaluation of a Hybrid Method of CFD and Prescribed Wake Model for Rotary Wings in Hover, ” the 2nd Asian/Australian Rotorcraft Forum and the 4th International Basic Research Conference on Rotorcraft Technology, 2013.

[4] YAMAHA RMAX http://www.yamaha-motor.co.jp/sky/rmax/

[5] Kanazaki, M., et. al., “Nacelle Chine Installation Based on Wind-Tunnel Test Using Efficient Global Optimization,” Transactions of the Japan Society for Aeronautical and Space Sciences, Vol. 51, No. 173, pp. 146–150, 2008.

[6] Kanazaki, M., et. al., “High-Lift System Optimization Based on Kriging Model Using High Fidelity Flow Solver, ” Transaction of Japan Society for Aeronautical and Space Science, Vol. 49, No. 165, pp. 169-174, 2006.

[7] Goldberg, D. E., “Genetic Algorithms in Search, Optimization & Machine Learning,” Addison-Wesley Publishing, Inc., Reading, 1989.

[8] Matthias, S., “Computer Experiments and Global Optimization,” Ph. D. Dissertation, Statistic and Actuarial Science Dept., University of Waterloo, 1997.

[9] Tanabe, Y. and Saito, S., “Significance of All-Speed Scheme in Application to Rotorcraft CFD Simulation,” the 3rd International Basic Research Conference on Rotorcraft Technology, 2009.

[10] Yamamoto, S. and Daiguji, H., “High-Order-Accurate Upwind Schemes for Solving the Compressible Euler and Navier-Stokes Equations, Computers & Fluids ,Vol.22, No2/3, pp.259-270, 1993.

[11] Zhang, L. P. and Wang, Z. J., “A block LU-SGS implicit dual time-stepping algorithm for hybrid dynamic meshes”, Computers & Fluids, Vol.33, pp.891-916, 2004.